Int J Clin Exp Med 2015;8(1):698-705
www.ijcem.com /ISSN:1940-5901/IJCEM0003908

Original Article

Superparamagnetic iron oxide promotes osteogenic differentiation of rat adipose-derived stem cells

Hai-Tao Xiao[1,2*], Lei Wang[1*], Bin Yu[1]

[1]Department of Orthopaedics and Traumatology, Nanfang Hospital, Southern Medical University, 1838 Guangzhou Avenue North, Guangzhou 510515, People's Republic of China; [2]Department of Traumatic Orthopaedics, Hainan Provincial People's Hospital, Haikou 570311, Hainan, People's Republic of China. [*]Equal contributors.

Received November 17, 2014; Accepted January 9, 2015; Epub January 15, 2015; Published January 30, 2015

Abstract: Adult adipose tissue-derived stem cells (ADSCs) were found to hold great promise for use in bone tissue repair and regeneration. The present study aims to improve the osteogenesis of ADSCs by Superparamagnetic Iron Oxide (SPIO), which is widely used in tissue imaging. In this study, adipose-derived stem cells were harvested from 4-week-old male Sprague-Dawley (SD) rats. The proliferation rates of ADSCs labeling with or without SPIO were assessed by using trypan blue assay. The osteogenic capability was examined by employing the ALP activity detection kit. The mineralization of cells was determined by staining with Alizarin red S. Flow cytometry analysis was used to examine the cell apoptosis treated with or without SPIO. Real-time reverse transcription polymerase chain reaction (RT-PCR) analysis was utilized to detect the Runx2, Opn, Ocn and ALP genes in the cells. The results indicated that SPIO could promote rat ADSCs proliferation and reduce rat ADSCs apoptosis. Also, SPIO could significantly enhance the ALP and alizarin red staining of ADSCs in -SPIO group and +SPIO group ($P < 0.01$). Furthermore, we also found that the expression of Runx2, Opn, Ocn and ALP was significantly increased after SPIO treatment compared to the un-treated cells ($P < 0.01$). In conclusion, SPIO could promote the osteogenic differentiation of rat adipose-derived stem cells, which would also become a great potential therapeutic tool in bone tissue engineering.

Keywords: Adipose derived stem cells, osteogenic differentiation, SPIO

Introduction

Large bone defects caused by extensive injury, congenital malformations or diseases, create a major challenge to orthopedic surgeons. Embryonic stem cells (ESCs), owning to their pluripotentiality, are more and more used in bone tissue regeneration [1-3]. But their practical use is limited due to ethical concerns and regulation [4]. Adipose derived stem cells (ADSCs) are easily and abundantly available and capable of differentiating into multiple mesenchymal cell types, such as adipocytes, chondrocytes, osteoblasts and myoblasts [5, 6] avoiding ESCs defects. Moreover, ADSCs have been extensively used for bone regeneration in various animal defect models, including craniofacial, tibial and mandibular defects, as well as some clinical trials [7-10]. ADSCs represent a kind of promising stem cells for bone tissue engineering.

Problems arise that localization and proliferation of the implanted ADSCs, as well as migration patterns between different organs, are critical parameters for evaluation of therapeutic efficacy [11] since improper cell homing and engraftment is recognized as a fundamental issue for cell-based therapies [12]. Therefore, being able to monitor the in vivo behavior of implanted MSCs and understand the fate of these cells is necessary for further development of successful therapies and requires an effective, non-invasive and non-toxic technique for cell tracking. Super paramagnetic iron oxide (SPIO) has broad applications in medicine, including use as a biosensor, in cell separation, cancer drug delivery, magnetic resonance imaging (MRI) and magnetic fluid hyperthermia (MFH) [13-15]. These characteristics make SPIO an ideal label and tracer for cell-based therapies and ADSCs can be labeled by SPIO with almost 100% efficiency with transfection

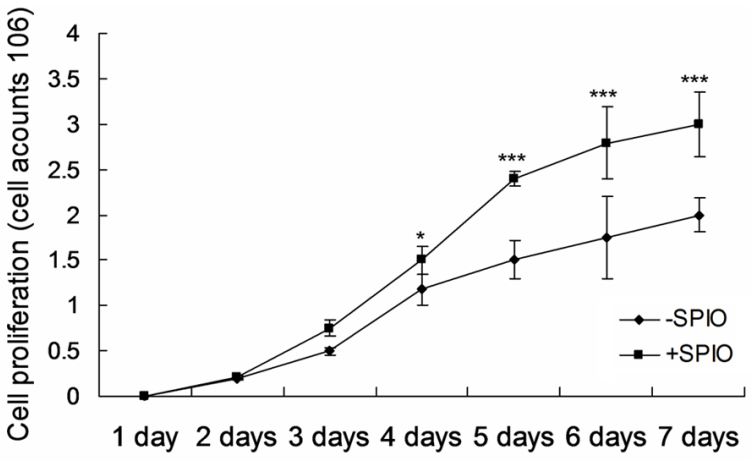

Figure 1. Growth curve of ADSCs cells proliferation. The statistical data indicates that SPIO promotes ADSCs proliferation. $^{*}P < 0.05$, $^{***}P < 0.001$ represent the cell proliferation of SPIO treated cells compared to without SPIO treated cells.

agent (TA) [16]. MRI can be used to follow SPIO-labeled MSCs and has been proposed as a gold standard for monitoring the in vivo biodistribution and migration of implanted SPIO-labeled MSCs [15].

The biological effects of SPIO-labeled MSCs administered with a TA have been investigated. SPIO labeling does not alter the morphological characteristics of MSCs and has no inhibitory effect on proliferation of MSCs from different sources [17]. Furthermore, labeling MSCs with ferumoxide does not adversely affect the functional properties of human BMSCs, and does not impair viability, long-term metabolic activity and chondrogenic differentiation [18]. However, SPIO labeling has been reported to promote human BMSC proliferation, which may be associated with cellular internalization of SPIO nanoparticles [19]. So far, whether SPIO labeling has effects on osteogenic differentiation of ADSCs has not been reported. In this study, we aim to examine the effect of SPIO on osteogenic differentiation of ADSCs and elucidate mechanisms that direct ADSC osteogenic differentiation.

Materials and methods

Animals

All animals and experimental procedures were approved by the local Institutional Animal Care and Use Committee complying with the "Guide for the Care and Use of Laboratory Animals" published by Southern Medical University.

Isolation of adipose-derived stem cells

Adipose-derived stem cells were harvested from 4-week-old male Sprague Dawley (SD) rats. The rats were killed by cervical dislocation and adipose tissue in the inguinal groove was isolated and washed extensively with equal volumes of phosphate-buffered saline (PBS) to remove blood cells. The isolated adipose tissue was then digested with 0.1% collagenase type I (Sigma Diagnostics Inc., St Louis, MO, USA) with intermittent shaking at 37°C for 30 min. The floating adipocytes were separated from the stromal cell fraction by centrifugation (300 g) for 5 min. The pellets were filtered through a 200 lm nylon mesh to remove cellular debris and incubated overnight at 37°C with 5% CO_2 in culture medium (high glucose DMEM (Hyclone), 10% fetal bovine serum (Invitrogen) and 100 U/mL penicillin/streptomycin (Invitrogen)). The primary cells were cultured for 4-5 days until they reached confluence and were defined as passage "0". The cells were passaged at a ratio of 1:3. The medium was changed every 2 days.

Proliferation assay

The proliferation rates of ADSCs labeling with or without SPIO were assessed by seeding 5×10^4 cells per well in 24-well culture plate with complete growth media. Trypan blue exclusion assay was performed on day 1, 2, 3, 4, 5, 6 and 7. A growth curve showing the number of viable cells versus days was plotted for each group.

Alkaline phosphatase (ALP) activity of ADSCs

The ADSCs were seeded in 6-well plates, and ALP activity was determined by staining with nitro blue tetrazolium (NBT) and 5-bromo-4-chroro-3-indolyl phosphate (BCIP). For quantification of ALP activity, cells seeded in 6-well plates were rinsed two times with phosphate-buffered saline (PBS), followed by trypsinization

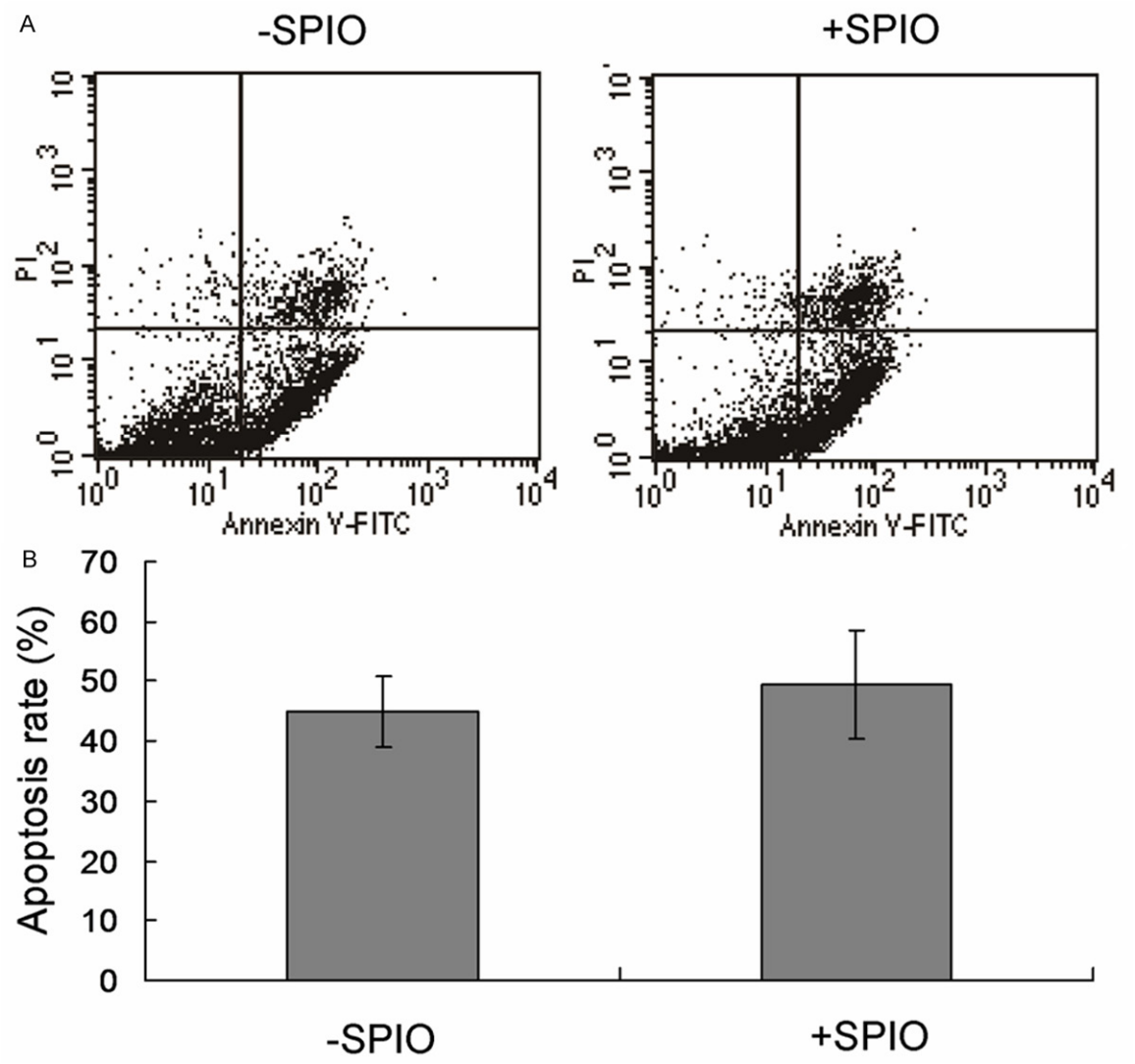

Figure 2. Flow cytometry analysis for apoptosis detection of the ADSCs cells. A. Flow cytometry analysis for SPIO treated and SPIO un-treated cells. B. Statistical analysis.

and then scraping in distilled water. This was followed by three cycles of freezing and thawing. ALP activity was determined at 405 nm using p-nitrophenyl phosphate (pNPP) as the substrate. Total protein contents were determined with the BCA method using the Pierce (Thermo Fisher Scientific, Rockford, IL, www.piercenet.com) protein assay kit in aliquots of the same samples, which were read at 562 nm and calculated against a series of bovine albumin (BSA) standards. Relative ALP activity to the control treatment was calculated after normalization to the total protein content.

Mineralization assays for ADSCs

The ADSCs were seeded in 6-well plates, and mineralization was determined by staining with Alizarin red S. To quantify matrix mineralization, Alizarin red S-stained cultures were incubated in 100 mM cetylpyridinium chloride for 1 h to solubilize and release calcium-bound Alizarin red S into the solution. The absorbance of the released Alizarin red S was measured at 562 nm. Relative Alizarin red S intensity to the control treatment was calculated after normalization to the total protein content.

Flow cytometry analysis for cell apoptosis

Cells were cultured in a six-well plate at 1 9 106 ells per well with complete DMEM in the presence or absence of a HDAC inhibitor NaBu (Sigma) that was dissolved in PBS, at indicated concentrations. After 72 h of culture, cells were harvested and washed three times in PBS.

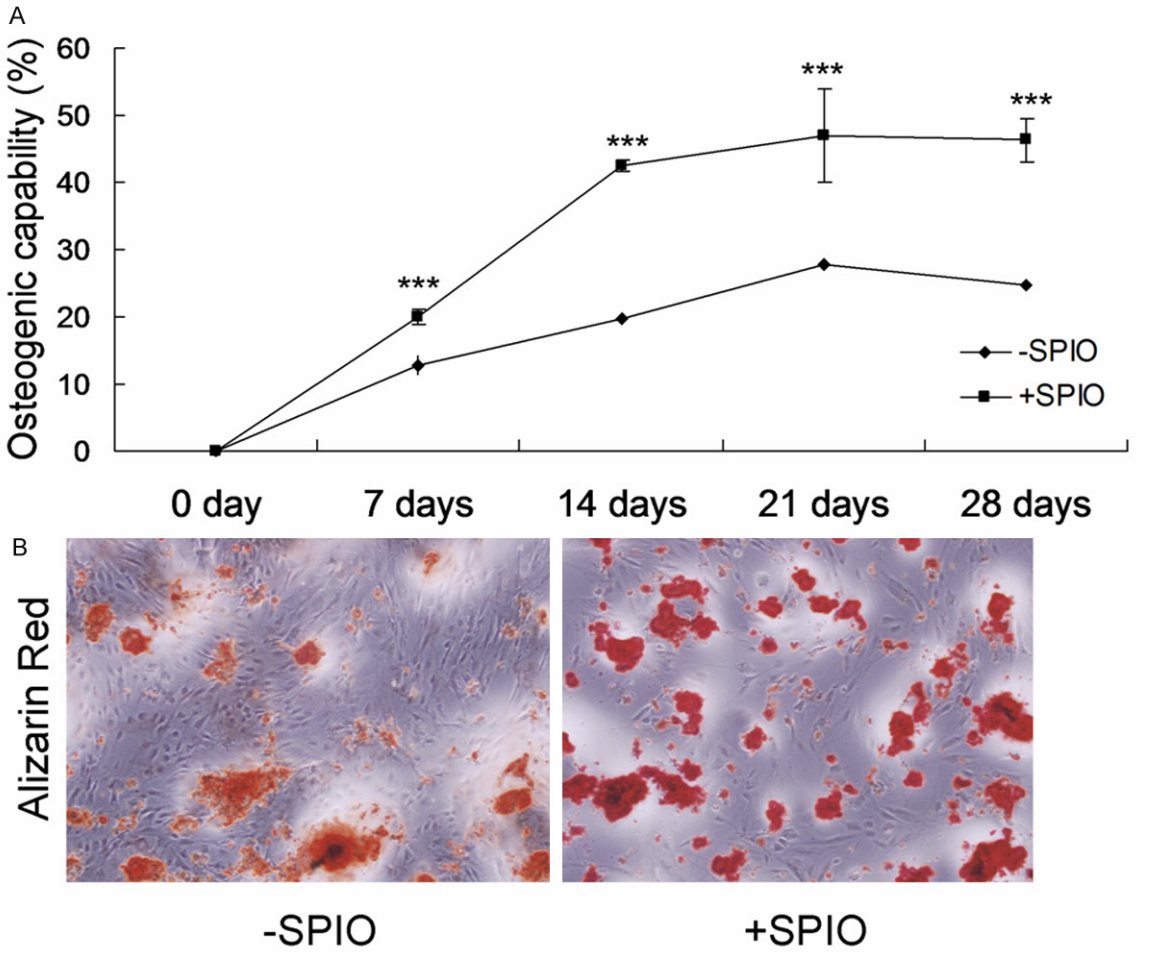

Figure 3. Osteogenic capability of the ADSCs treated with or without SPIO. A. ALP staining for the osteogenic capability. B. Alizarin red staining for the osteogenic capability. ***P < 0.001 represent the osteogenic capability of SPIO treated cells compared to without SPIO treated cells.

Cells from each sample were processed for Annexin V fluorescein isothiocyanate (FITC)/ propidium iodide (PI) apoptosis detection (Becton Dickinson, Franklin Lakes, NJ, USA) according to the manufacturer's instructions. All experiments were carried out in triplicate and repeated three times.

Real-time reverse transcription polymerase chain reaction (RT-PCR) analysis

Cells were seeded into a six-well plate at 1 9 105 cells per well and harvested at assigned time points post induction. Total RNA extraction was performed using Trizol Reagent (Invitrogen, Carlsbad, CA, USA) based on the manufacturer's instructions. Amplifications were performed with the ABI 7300 Real-Time PCR System (ABI, Carlsbad, CA, USA) with different primers. The primers used were as follows: Runx2 forward TCCAGACCAGCAGCACTCC and reverse TCAGCGTCAACACCATCATTC; osteopontin (Opn) forward AATGAAGGGCCCTGAGC and reverse GCCAGTTCTGCAAGGAAGC; osteocalcin (Ocn) forward AACGGTGGTGCCATAGATGC and reverse AGGACCCTCTCTCTGCTCAC; ALP forward CCAGCAGGCTTACCAAGAA and reverse TTTATCGCACAAAGGGAACA; 18 S rRNA forward GTAACCCGTTGAACCCCATT and reverse CCATCCAATCGGTAGTAGCG. All annealing temperatures were set at 60°C. Transcription levels were normalized to GAPDH mRNA level. Each value represents the average of at least three independent experiments.

Statistical analysis

The results are expressed as means standard deviation (SD). Comparisons between groups were analyzed using Student's t-test or analysis

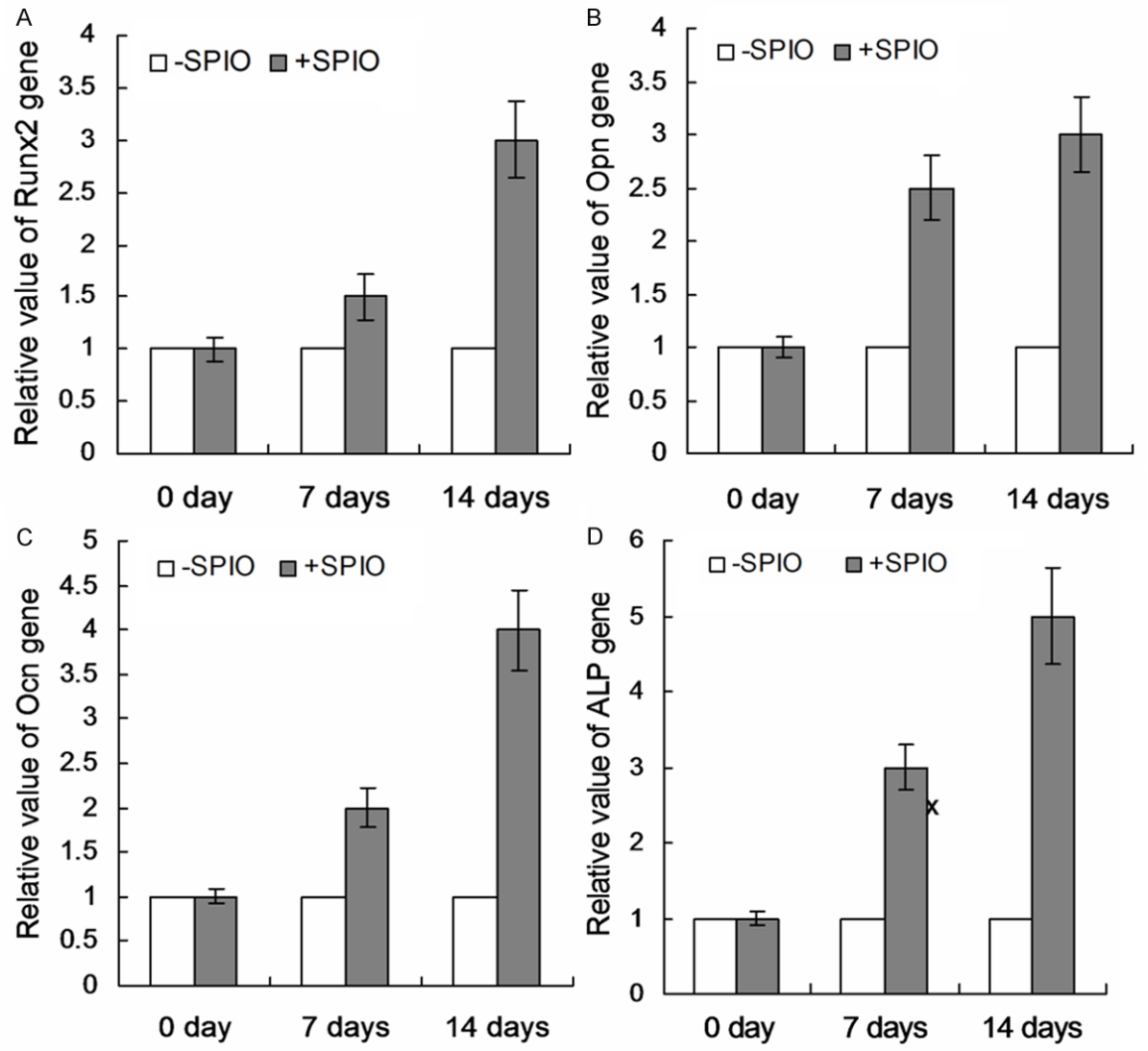

Figure 4. Effects of SPIO treatment on the expression of osteogenic genes. Relative expression of osteogenic gene Runx2 (A), Opn (B), Ocn (C) and ALP (D) were analyzed and calculated.

of variance (ANOVA), and the Student-Newman-Kleuss method was used to estimate the level of significance. Differences were considered to be statistically significant at $P < 0.05$.

Results

SPIO labeling could enhance ADSCs proliferation

Adipose-derived stem cells isolated from the inguinal groove adipose tissue of 4-week-old rats were initially plated in cell culture dishes (diameter 100 mm). Adipose-derived stem cells at the third passage became more uniform and grew in a monolayer with typical fibroblast morphology. All characterizations were performed on the cells at passage 3. Flow cytometry results showed that the ADSCs consisted of a single phenotypic population positive for CD44 (99.51%) and CD90 (99.73%).

Then, we labeled ADSCs with or without SPIO. Through series observation, we found that, when labeled with SPIO, ADSCs growth rate was fast than their controls (**Figure 1**), and ADSCs apoptosis was not changed (**Figure 2A** and **2B**).

Effect of SPIO labeling on osteogenic differentiation of ADSCs

We showed above that SPIO labeling could promote proliferation of ADSCs. We then continue

to assess whether SPIO labeling has effect on osteogenic differentiation of ADSCs. ADSCs were first labeled with or without SPIO for 2 days and then induced by osteogenic differentiation medium. As shown in **Figure 3A** and **3B**, SPIO labeling could significantly enhance the ALP and alizarin red staining of ADSCs, suggesting that SPIO labeling significantly increased osteogenic differentiation capacity of ADSCs.

SPIO enhances the expression of osteogenic genes

SPIO could increase ADSCs osteogenic differentiation promotes us to further examine the mechanism. We found that the expression of Runx2, Opn, Ocn and ALP (**Figure 4A-D**) were significantly increased after SPIO labeling.

Discussion

The biological effects of SPIO-labeled other stem cells have been reported, but the biological effects of SPIO-labeled ADSCs administered with a TA have not been reported yet. In our study, we showed that SPIO-labeled ADSCs showed increased cell proliferation and accelerated osteogenic differentiation. And the phenotypes may be related with up-regulated expression of osteogenic genes, such as Runx2, Opn, Ocn and ALP.

Reports have been showed that SPIO labeling does not alter the morphological characteristics of MSCs and has no inhibitory effect on proliferation of MSCs from different sources [20-25]. The viability and proliferation of rat BMSCs is unaffected by intra-cytoplasmic SPIO. In rat MSCs, no significant differences were observed between unlabeled and SPIO-labeled cells in terms of viability, proliferation, membranous antigen and pluripotency into multiple lineages [18]. In fact, SPIO labeling has been reported to promote human BMSC proliferation [26, 27], which may be associated with cellular internalization of SPIO nanoparticles [26]. In ADSCs, we also found that, SPIO could increase the proliferation of ADSCs. However, excess quantities of divinyl-coated SPIO inhibited the proliferation of MSCs [28].

Adipogenic and osteogenic differentiation of MSCs was not affected by SPIO labeling in most studies ([17, 29-32]. However, SPIO labeling did dose-dependently interfere with osteogenic differentiation of human BMSCs, likely due to the production of Fe from the labeling reaction, which could activate cellular signaling and inhibit osteogenesis [33, 34]. In our study, we also found that the same effect. SPIO-labeled ADSCs showed increased osteogenic differentiation, which may be related with up-regulated expression of osteogenic genes, such as Runx2, Opn, Ocn and ALP. Our data showed great promise of ADSCs in bone tissue engineering.

Acknowledgements

This work was supported by Department of Orthopaedics and Traumatology, Nanfang Hospital, Southern Medical University, China.

Disclosure of conflict of interest

None.

Address correspondence to: Dr. Bin Yu, Department of Orthopaedics and Traumatology, Nanfang Hospital, Southern Medical University, 1838 Guangzhou Avenue North, Guangzhou 510515, People's Republic of China. Tel: +86-20-61641746; Fax: +86-20-61641746; E-mail: binyu0001@yeah.net

References

[1] Song Q, Xu R, Zhang Q, Ma M, Zhao X. Therapeutic effect of transplanting bone mesencymal stem cells on the hind libms' motor function of rats with acute spinal cord injury. Int J Clin Exp Med 2014; 7: 262-267.

[2] Marolt D, Campos IM, Bhumiratana S, Koren A, Petridis P, Zhang G, Spitalnik PF, Grayson WL, Vunjak-Novakovic G. Engineering bone tissue from human embryonic stem cells. Pro Nat Acad Sci U S A 2012; 109: 8705-8709.

[3] Kim MJ, Park JS, Kim S, Moon SH, Yang HN, Park KH, Chung HM. Encapsulation of bone morphogenic protein-2 with Cbfa1-overexpressing osteogenic cells derived from human embryonic stem cells in hydrogel accelerates bone tissue regeneration. Stem Cells Dev 2011; 20: 1349-1358.

[4] Chen X, Gu Q, Wang X, Ma Q, Tang H, Yan X, Guo X, Yan H, Hao J, Zeng F. Directed neuronal differentiation of mouse embryonic and induced pluripotent stem cells and their gene expression profiles. Int J Mol Med 2013; 32: 25-34.

[5] Choudhery MS, Badowski M, Muise A, Harris DT. Comparison of human mesenchymal stem cells derived from adipose and cord tissue. Cytotherapy 2013; 15: 330-343.

[6] Meric A, Yenigun A, Yenigun VB, Dogan R, Ozturan O. Comparison of chondrocytes produced from adipose tissue-derived stem cells and cartilage tissue. J Craniofac Surg 2013; 24: 830-833.
[7] Szepes M, Benko Z, Cselenyak A, Kompisch KM, Schumacher U, Lacza Z, Kiss L. Comparison of the direct effects of human adipose- and bone-marrow-derived stem cells on post-ischemic cardiomyoblasts in an in vitro simulated ischemia-reperfusion model. Stem Cells Int 2013; 2013: 178346.
[8] Ong WK, Sugii S. Adipose-derived stem cells: fatty potentials for therapy. Int J Biochem Cell Biol 2013; 45: 1083-1086.
[9] McLaughlin MM, Marra KG. The use of adipose-derived stem cells as sheets for wound healing. Organogenesis 2013; 9: 79-81.
[10] Marycz K, Smieszek A, Grzesiak J, Donesz-Sikorska A, Krzak-Ros J. Application of bone marrow and adipose-derived mesenchymal stem cells for testing the biocompatibility of metal-based biomaterials functionalized with ascorbic acid. Biomed Mater 2013; 8: 065004.
[11] Yu S, Zhu Y, Li F, Zhang Y, Xia C. Differentiation of human embryonic germ cells and transplantation in rats with acute myocardial infarction. Exp Ther Med 2014; 7: 615-620.
[12] Hassan WU, Greiser U, Wang W. Role of adipose-derived stem cells in wound healing. Wound Repair Regen 2014; 22: 313-325.
[13] Nishie A, Tajima T, Ishigami K, Ushijima Y, Okamoto D, Hirakawa M, Nishihara Y, Taketomi A, Hatakenaka M, Irie H. Detection of hepatocellular carcinoma (HCC) using super paramagnetic iron oxide (SPIO)-enhanced MRI: Added value of diffusion-weighted imaging (DWI). J Magn Reson Imaging 2010; 31: 373-382.
[14] Feng X, Gao F, Zheng Y. Thermally modulated photoacoustic imaging with super-paramagnetic iron oxide nanoparticles. Opt Lett 2014; 39: 3414-3417.
[15] Qi Y, Feng G, Huang Z, Yan W. The application of super paramagnetic iron oxide-labeled mesenchymal stem cells in cell-based therapy. Mol Biol Rep 2013; 40: 2733-2740.
[16] Rice HE, Hsu EW, Sheng H, Evenson DA, Freemerman AJ, Safford KM, Provenzale JM, Warner DS, Johnson GA. Superparamagnetic iron oxide labeling and transplantation of adipose-derived stem cells in middle cerebral artery occlusion-injured mice. AJR Am J Roentgenol 2007; 1101-1108.
[17] Arbab AS, Bashaw LA, Miller BR, Jordan EK, Lewis BK, Kalish H, Frank JA. Characterization of biophysical and metabolic properties of cells labeled with superparamagnetic iron oxide nanoparticles and transfection agent for cellular MR imaging. Radiology 2003; 229: 838-846.
[18] Sun JH, Zhang YL, Qian SP, Yu XB, Xie HY, Zhou L, Zheng SS. Assessment of biological characteristics of mesenchymal stem cells labeled with superparamagnetic iron oxide particles in vitro. Mol Med Rep 2012; 5: 317-320.
[19] Yu X, Lu C, Liu H, Rao S, Cai J, Liu S, Kriegel AJ, Greene AS, Liang M, Ding X. Hypoxic preconditioning with cobalt of bone marrow mesenchymal stem cells improves cell migration and enhances therapy for treatment of ischemic acute kidney injury. PLoS One 2013; 8: e62703.
[20] Kraitchman DL, Tatsumi M, Gilson WD, Ishimori T, Kedziorek D, Walczak P, Segars WP, Chen HH, Fritzges D, Izbudak I. Dynamic imaging of allogeneic mesenchymal stem cells trafficking to myocardial infarction. Circulation 2005; 112: 1451-1461.
[21] Schafer R, Bantleon R, Kehlbach R, Siegel G, Wiskirchen J, Wolburg H, Kluba T, Eibofner F, Northoff H, Claussen CD, Schlemmer HP. Functional investigations on human mesenchymal stem cells exposed to magnetic fields and labeled with clinically approved iron nanoparticles. BMC Cell Biol 2010; 11: 22.
[22] Arbab AS, Yocum GT, Kalish H, Jordan EK, Anderson SA, Khakoo AY, Read EJ, Frank JA. Efficient magnetic cell labeling with protamine sulfate complexed to ferumoxides for cellular MRI. Blood 2004; 104: 1217-1223.
[23] Qiu Y, Yun MM, Han X, Zhao R, Zhou E, Yun S. Human umbilical cord mesenchymal stromal cells suppress MHC class II expression on rat vascular endothelium and prolong survival time of cardiac allograft. Int J Clin Exp Med 2014; 7: 1760-1767.
[24] Heymer A, Haddad D, Weber M, Gbureck U, Jakob PM, Eulert J, Noth U. Iron oxide labelling of human mesenchymal stem cells in collagen hydrogels for articular cartilage repair. Biomaterials 2008; 29: 1473-1483.
[25] Zeng G, Wang G, Guan F, Chang K, Jiao H, Gao W, Xi S, Yang B. Human amniotic membrane-derived mesenchymal stem cells labeled with superparamagnetic iron oxide nanoparticles: the effect on neuron-like differentiation in vitro. Mol Cell Biochem 2011; 357: 331-341.
[26] Chang YK, Liu YP, Ho JH, Hsu SC, Lee OK. Amine-surface-modified superparamagnetic iron oxide nanoparticles interfere with differentiation of human mesenchymal stem cells. J Orthop Res 2012; 30: 1499-1506.
[27] Huang DM, Hsiao JK, Chen YC, Chien LY, Yao M, Chen YK, Ko BS, Hsu SC, Tai LA, Cheng HY. The promotion of human mesenchymal stem cell proliferation by superparamagnetic iron oxide nanoparticles. Biomaterials 2009; 30: 3645-3651.
[28] Hinds KA, Hill JM, Shapiro EM, Laukkanen MO, Silva AC, Combs CA, Varney TR, Balaban RS,

Koretsky AP, Dunbar CE. Highly efficient endosomal labeling of progenitor and stem cells with large magnetic particles allows magnetic resonance imaging of single cells. Blood 2003; 102: 867-872.

[29] Farrell E, Wielopolski P, Pavljasevic P, van Tiel S, Jahr H, Verhaar J, Weinans H, Krestin G, O'Brien FJ, van Osch G, Bernsen M. Effects of iron oxide incorporation for long term cell tracking on MSC differentiation in vitro and in vivo. Biochem Biophy Research Commun 2008; 369: 1076-1081.

[30] Frank JA, Miller BR, Arbab AS, Zywicke HA, Jordan EK, Lewis BK, Bryant LH, Bulte JW. Clinically applicable labeling of mammalian and stem cells by combining superparamagnetic iron oxides and transfection agents. Radiology 2003; 228: 480-487.

[31] Schafer R, Ayturan M, Bantleon R, Kehlbach R, Siegel G, Pintaske J, Conrad S, Wolburg H, Northoff H, Wiskirchen J, Weissert R. The use of clinically approved small particles of iron oxide (SPIO) for labeling of mesenchymal stem cells aggravates clinical symptoms in experimental autoimmune encephalomyelitis and influences their in vivo distribution. Cell Transplant 2008; 17: 923-941.

[32] Schafer R, Kehlbach R, Muller M, Bantleon R, Kluba T, Ayturan M, Siegel G, Wolburg H, Northoff H, Dietz K. Labeling of human mesenchymal stromal cells with superparamagnetic iron oxide leads to a decrease in migration capacity and colony formation ability. Cytotherapy 2009; 11: 68-78.

[33] Chen YC, Hsiao JK, Liu HM, Lai IY, Yao M, Hsu SC, Ko BS, Chen YC, Yang CS, Huang DM. The inhibitory effect of superparamagnetic iron oxide nanoparticle (Ferucarbotran) on osteogenic differentiation and its signaling mechanism in human mesenchymal stem cells. Toxicol Appl Pharmacol 2010; 245: 272-279.

[34] Kim BS, Kim HJ, Kim JS, You YO, Zadeh H, Shin HI, Lee SJ, Park YJ, Takata T, Pi SH, Lee J, You HK. IFITM1 increases osteogenesis through Runx2 in human alveolar-derived bone marrow stromal cells. Bone 2012; 51: 506-514.